実験報告書様式（一般利用課題・成果公開利用）

（ ※本報告書は英語で記述してください。ただし、産業利用課題として採択されている方は日本語で記述していただいても結構です。 ）

MLF Experimental Report

J-PARC **MLF Experimental Report**	提出日 Date of Report **2017/08/21**
課題番号 Project No. **2014A0280** 実験課題名 Title of experiment On the crystal perfection and defect kinetics in the high temperature phases of Zr, Ti and Al alloys: An in-situ study of primary extinction 実験責任者名 Name of principal investigator Klaus-Dieter Liss 所属 Affiliation Australian Nuclear Science and Technology Organisation	装置責任者 Name of responsible person Stefanus Harjo, Kazuya Aizawa 装置名 Name of Instrument/（BL No.） TAKUMI / BL19 実施日 Date of Experiment 2014/05/03 9:00-2015/05/08 9:00 experimental team Klaus-Dieter Liss, Pingguang Xu, Stefanus Harjo, Kazuya Aizawa, Wu Gong, Takiro Kawasaki; (samples: Eitaro Yukutake; Bob Harrison)

試料、実験方法、利用の結果得られた主なデータ、考察、結論等を、記述して下さい。（適宜、図表添付のこと）

Please report your samples, experimental method and results, discussion and conclusions. Please add figures and tables for better explanation.

1. 試料 Name of sample(s) and chemical formula, or compositions including physical form.

Experiment ID and run numbers are listed in Table 1 and the run date in Figure 1.

exID	runNo	sample_name
5296	22262	Zr_2.5Nb
5297	22263	A2011_Sample6
5298	22264	Ti_Grade2_T3
5299	22265	Al1370_Sample-B
5300	22266	Ti-grade2-T1-run1
5301	22267	Ti-grade2-T4-run1
5302	22268	Ti-grade2-T2-run1
5303	22269	Ti6Al4V-run1
5304	22270	Zr-2.5Nb-sample4-run1
5305	22271	Zr-2.5Nb-sample4-run1
5306	22272	Zr-2.5Nb-sample6-run1
5307	22273	Ti-grade2-T5_run1
5308	22274	Ti-grade2-T5_run1
5309	22275	Al-1370-PartC_run1
	22249	Vanadium-pattern

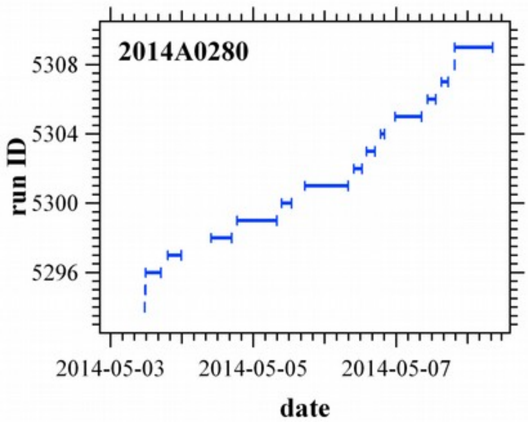

Figure 1: Experiment ID displayed along experimental time showing effective usage of the beam time.

Table 1 (left)

2. 実験方法及び結果（実験がうまくいかなかった場合、その理由を記述してください。）

Experimental method and results. If you failed to conduct experiment as planned, please describe reasons.

Goal of the experiment was to obtain the defect kinetics in materials at very high temperature, where crystallites anneal to become perfect crystals, and upon mechanical distortion by plastic deformation. We use the transition between the kinematic and

dynamical theory of diffraction, where primary extinction of radiation plays a role. Upon heating, dislocations annihilate showing a decrease of intensity. Upon plastic deformation, the intensity restores due to the introduction of strain fields. Similar distortions are formed when a second phase precipitates. Furthermore, microstructural and crystallographic parameters can be extracted from the recorded diffractograms, reflecting in various parameters, namely peak position G, shape, e.g. width ΔH and intensity R. Upon heating and cooling, typical lattice strain $\varepsilon = -\Delta G/G$ is dominated by linear thermal expansion, change of phase composition, order parameter and relaxation of residual stresses.
Tensile specimens listed in Table 1 have been fabricated and measured in-situ in the load-frame upon a heating, plastic deformation and cooling process. The sample axis has been mounted in diagonal axis such that the integrated detector arrays 0001 and 0000 probe for scattering vectors in longitudinal and transverse direction according to **L** = 南 = SOUTH = 0001 and **T** = 北 = NORTH = 0000, respectively.
The provided vanadium pattern for each detector bench have been fitted by 16th-order polynomials in order to smoothen the counting statistics, which then were taken to normalize each measured time-of-flight diffraction pattern channel by channel. The instrument was calibrated to be momentum transfer $Q = 2\pi$ / (TOF/15000), where TOF is the time-of-flight channel number in the data collection. Load-frame processing data were stored in adjacent ASCII data files with ending *.CSV.

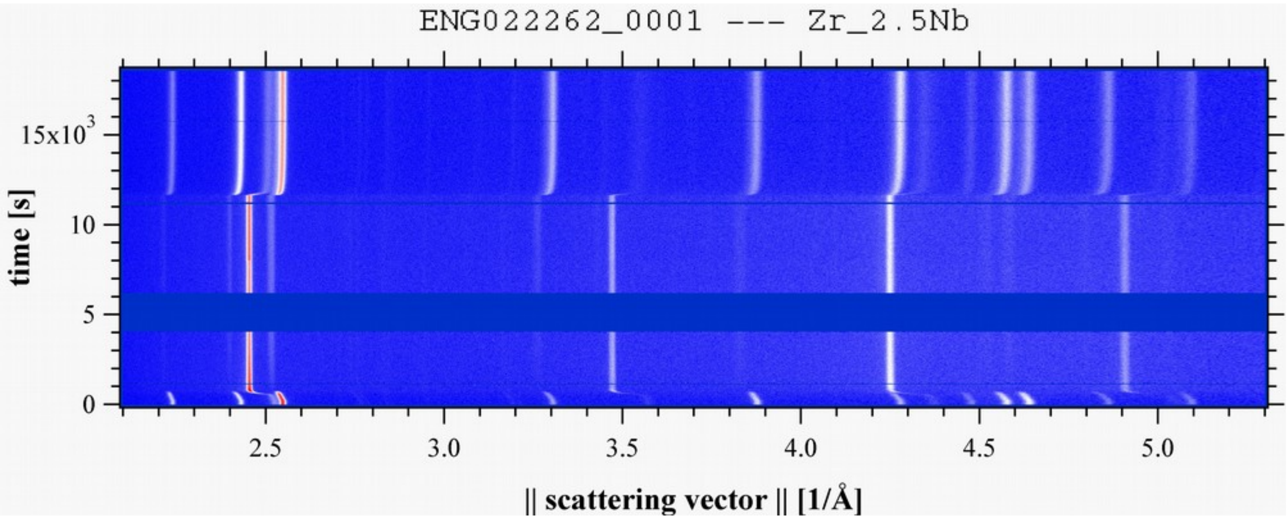

Figure 2: Representative specimen-run after normalization and calibration.

The run on Zr-2.5Nb shown in Figure 2 shows the $\alpha \rightarrow \beta$ phase transformation in Zr-2.5Nb with a strong β-110 reflection appearing at 2.45 Å^{-1}. Upon holding, it can be recognized that its intensity slowly decreases due to increasing crystal perfection by annihilation of dislocations and microstructure recovery. At around 8 ks, the reflectivity suddenly increases due to plastic deformation undertaken at this time, which introduces defects, followed again by subsequent recovery. The remaining α- and other β-reflections do not show this behavior because their extinction length is larger than the size of the crystallites, therefore scattering all the time kinematically. Zr alloys demonstrate best this behavior. In Ti, recovery has been found to be almost too fast to follow, and Al exposes more intensity changes by texture, hiding this recovery effect.
KDL is actually taking up an academic university appointment, and will focus on this topic for further data analysis and microstructure observation and modeling, aiming for the early academic publication.